Low Light Adaptation: Energy Transfer Processes in Different Types of Light Harvesting Complexes from *Rhodopseudomonas palustris*

Vladimíra Moulisová,[†] Larry Luer,[‡§] Sajjad Hoseinkhani,[‡] Tatas H. P. Brotosudarmo,[†] Aaron M. Collins,[¶] Guglielmo Lanzani,[‖] Robert E. Blankenship,[¶] and Richard J. Cogdell[†*]

[†]Faculty of Biomedical and Life Sciences, University of Glasgow, Glasgow, United Kingdom; [‡]CNR/INFM ULTRAS, Department of Physics, Politecnico di Milano, Milan, Italy; [§]IMDEA Nanociencia, Facultad de Ciencias, Módulo C-IX, Ciudad Universitaria de Cantoblanco, Madrid, Spain; [¶]Departments of Biology and Chemistry, Washington University in St. Louis, St. Louis, Missouri; and [‖]Italian Institute of Technology and Department of Physics, Politecnico di Milano, Milan, Italy

ABSTRACT Energy transfer processes in photosynthetic light harvesting 2 (LH2) complexes isolated from purple bacterium *Rhodopseudomonas palustris* grown at different light intensities were studied by ground state and transient absorption spectroscopy. The decomposition of ground state absorption spectra shows contributions from B800 and B850 bacteriochlorophyll (BChl) *a* rings, the latter component splitting into a low energy and a high energy band in samples grown under low light (LL) conditions. A spectral analysis reveals strong inhomogeneity of the B850 excitons in the LL samples that is well reproduced by an exponential-type distribution. Transient spectra show a bleach of both the low energy and high energy bands, together with the respective blue-shifted exciton-to-biexciton transitions. The different spectral evolutions were analyzed by a global fitting procedure. Energy transfer from B800 to B850 occurs in a mono-exponential process and the rate of this process is only slightly reduced in LL compared to high light samples. In LL samples, spectral relaxation of the B850 exciton follows strongly nonexponential kinetics that can be described by a reduction of the bleach of the high energy excitonic component and a red-shift of the low energetic one. We explain these spectral changes by picosecond exciton relaxation caused by a small coupling parameter of the excitonic splitting of the BChl *a* molecules to the surrounding bath. The splitting of exciton energy into two excitonic bands in LL complex is most probably caused by heterogenous composition of LH2 apoproteins that gives some of the BChls in the B850 ring B820-like site energies, and causes a disorder in LH2 structure.

INTRODUCTION

Absorption of solar energy by photoactive pigments and energy transfer through a cascade of antenna complexes to the photosynthetic reaction center (RC) represent the earliest reactions in photosynthesis. In purple photosynthetic bacteria, there are two main types of light harvesting complexes, LH1 and LH2 (1). The crystal structures of a few of these LH complexes isolated from purple nonsulfur bacteria have been solved by x-ray crystallography, e.g., the LH2 complex from *Rhodopseudomonas* (*Rps.*) *acidophila* 10050 (2), the LH2 from *Rhodospirillum molischianum* (3), the LH3 (LH2 version from low light) from *Rps. acidophila* 7050 (4) and the LH1-RC complex (core-complex, LH1 with photosynthetic reaction center) from *Rhodopseudomonas palustris* (5). The LH2 complex from *Rps. acidophila* consists of nine α- and β-apoprotein dimers arranged in a highly symmetric ring. Each heterodimer binds three BChl *a* molecules, one which is monomeric and two of which are strongly coupled. The overall complex contains nine monomeric and 18 strongly coupled BChl *a* molecules. The nine monomeric BChls absorb in the NIR at 800 nm and are called B800, the 18 tightly coupled BChls absorb at 850 nm (B850). The LH1 complex isolated from the *Rps. palustris* consists of 15 α/β-heterodimer subunits that form an ellipse that surrounds the RC. LH1 only has the tightly coupled BChl *a* molecules absorbing at 875 nm (B875). Light energy absorbed by B800 is transferred to B850, then on to B875 in LH1 from where it is finally transferred to BChls in RC (6).

The knowledge of these structures has allowed the energy transfer (ET) processes that take place in and between them to be understood in great detail (7). It has been found that some purple bacteria adapt to growth at lower light intensities by synthesizing LH complexes with modified spectral properties (8). It is not yet clear what the differences are in the ET processes taking place in these complexes in comparison to their high light (HL) counterparts. When growing at low light (LL) intensities, the bacterium *Rps. palustris* changes the spectral properties of its LH2 complexes. Compared to the HL form of LH2 the absorption spectrum of LL LH2 complexes has a lower, broader absorption at 850 nm and a broader, relatively higher absorption peak at 800 nm (9,10). Tadros et al. (11) and Tadros and Waterkamp (12) identified multiple genes encoding LH2 α- and β-apoproteins in *Rps. palustris*. Different members of this multigene family are expressed depending on the growth conditions (13,14). It has also been shown that both the HL and LL LH2 complexes from *Rps. palustris* contain multiple antenna apoprotein types, suggesting the possibility of LH2 rings with mixed populations of polypeptides giving different spectral properties to B850 BChls (15). This idea was supported by a resonance Raman spectroscopy study on LL LH2 complexes,

Submitted July 24, 2009, and accepted for publication September 10, 2009.

*Correspondence: gbta18@udcf.gla.ac.uk

Editor: Leonid S. Brown.

0006-3495/09/12/3019/10 $2.00

doi: 10.1016/j.bpj.2009.09.023

where in B850 ring B820-like characteristics were observed beside B850-like BChls (16). The CD spectrum of the LL LH2 complexes also showed an additional band located at ~820 nm compared with HL LH2 (17,18).

At the time of writing, few time-resolved studies have looked at the energy transfer reactions that take place within the LL LH2 complexes from *Rps. palustris*. Hess et al. (19) described the energy transfer in bacterial membranes isolated from *Rps. palustris* grown at low light conditions measured by picosecond pump probe spectroscopy. A more detailed transient spectroscopic study on extensively purified LL LH2 complexes was conducted by Nishimura and colleagues who found a B824 component and suggested several possible kinetic models for the energy transfer pathways present (20). This study is focused on a detailed analysis of femtosecond pump-probe spectra obtained from LH2 samples isolated from *Rps. palustris* grown at four different light intensities, as well as on the analysis of their ground state absorption spectra. Recently, direct evidence has been found for the presence of BChl *a* molecules with both B850 and B820 site energies in individual LL LH2 complexes from *Rps. palustris* by use of single molecule spectroscopy (21). This information has been used to help interpret the data from this study and explain the ongoing specific spectral changes in LH2 complexes during low light adaptation.

MATERIALS AND METHODS

Bacteria growth conditions

Cells of *Rps. palustris* strain 2.1.6. were grown photoheterotrophically in Böse medium (22) at 30°C in flat-sided glass bottles. Four different light intensities were used: 220 Lux for HL and 10 Lux for LL, and two intermediate intensities, 90 Lux for intermediate 1 low light (LL1) and 20 Lux for intermediate 2 low light (LL2). The light was provided by incandescent bulbs, all the LL conditions were obtained by moving the cultures further away from the light source with the same spectral composition.

Membrane isolation and purification of LH2 complexes

Cell cultures were harvested and LH2 complexes isolated and purified from photosynthetic membranes as described previously (23). Briefly, cells were harvested, homogenized, and disrupted by passage through a French press. Broken membranes were collected by differential centrifugation. They were then solubilized in 2% of LDAO and the core LH1/RC and LH2 complexes were separated by sucrose gradient centrifugation. The LH2 complexes were further purified by anion exchange chromatography (DE52 exchanger, Whatman International Ltd., Maidstone, UK) and gel filtration. Samples were kept frozen (−20°C) until used.

Steady-state absorption measurements

For steady-state spectroscopy, concentrated LH2 samples were mixed in buffer containing 0.1% LDAO in Tris-HCl (20 mM, pH 8.0), and for low temperature measurements, glycerol was added to a final concentration 66%. Low temperatures were obtained by the use of a liquid nitrogen cryostat (OptistatDN, Oxford Instruments, Bucks, UK). Absorption spectra were recorded using a PerkinElmer, Lambda 950 spectrophotometer (Waltham, Massachusetts).

Transient absorption measurements

The transient absorption difference $\Delta A/A$ spectra were recorded using a conventional pump-probe set-up (24). The ultrafast spectroscopy configuration used in these experiments started with a regeneratively amplified mode-locked Ti:Sapphire laser (Clark-MXR Inc., Dexter, Michigan) delivering pulses at 1 kHz repetition rate with 790 nm center wavelength, 150 fs duration, and 500 μJ energy. The pump energy was reduced to 50 nJ (0.03 mJ cm^{-2}). A fraction of the pulse energy was focused onto a thin sapphire plate to generate the white light broadband probe pulse. The NIR range from 790 to 950 nm was used. The pump pulse was provided by the driver laser, its second harmonic or an optical parametric amplifier. We used the NIR part of white light as a probe and fundamental wavelength of Ti:Sapphire laser as pump. The pump beam was modulated at 500 Hz by a mechanical chopper. After the probe pulse has traversed the sample, a two-dimensional $\Delta A/A$ readout as a function of pump-probe delay time was measured using optical multichannel analyzer in a single shot configuration. The chirp of the white light supercontinuum has been corrected for in the displayed spectra as described previously (24).

Global analysis

The global fitting procedure was carried out by minimizing the square of the error between the measured matrix, $\Delta A_{\mathrm{exp}}(E,t)$ and the calculated one, $\Delta A_{\mathrm{calc}}(E,t) = d \times \sum_i \sigma(i,E) \times c(i,t)$, by optimizing the absorption cross-sections $\sigma(i,E)$ and the populations $c(i,t)$ for all photoexcitations P_i, as defined in a standard kinetic equation scheme of the form $GS \overset{\mathrm{pump}}{\rightarrow} P_1 \overset{k_1(t)}{\rightarrow} P_2 \overset{k_2(t)}{\rightarrow} [P_3 \overset{k_3(t)}{\rightarrow}] GS$, where GS refers to the molecules in the ground state. The optimization is done iteratively by varying $k_i(t); i \in \{1,2,3\}$, whereas at each iteration step, $\sigma(i,E)$ is found by a Gaussian elimination. The sheet thickness is given by d. This approach is a generalization of the method described by van Stokkum and colleagues (25) where time-dependent rate constants have been included.

RESULTS AND DISCUSSION

Analysis of ground state absorption spectra

The ground state NIR absorption spectra of the LH2 complexes were measured at 77 K and 293 K (Fig. 1, *left* and *right columns*, respectively). Common features are observed in all spectra. At 1.55 eV, there is a relatively sharp absorption band with a vibronic replica at 1.62 eV. Both of these can be assigned to the Q_y band of the BChl *a* molecules in the B800 ring (26). At lower energy, there is a broader transition the position of which is clearly temperature dependent: 1.43 eV at 77 K, and 1.45 eV at 293 K. This transition is labeled Γ_{1L} and can be assigned to the transition from the ground state to the low energy one-exciton band of the B850 ring (26). The thermally induced blue-shift of Γ_{1L} can be explained by a temperature-induced weakening of the excitonic interaction, and hence a reduction of exciton splitting. Recently, similar temperature dependence of B850 blue-shift was observed in LH2 complexes from other bacteria when studied in the framework of the modified Redfield theory (27).

Growth of the bacterium under reduced illumination leads to characteristic changes in the ground state absorption spectra: Γ_{1L} loses oscillator strength, whereas the B800 band apparently becomes stronger and larger. This progression holds for both low and high temperature measurements

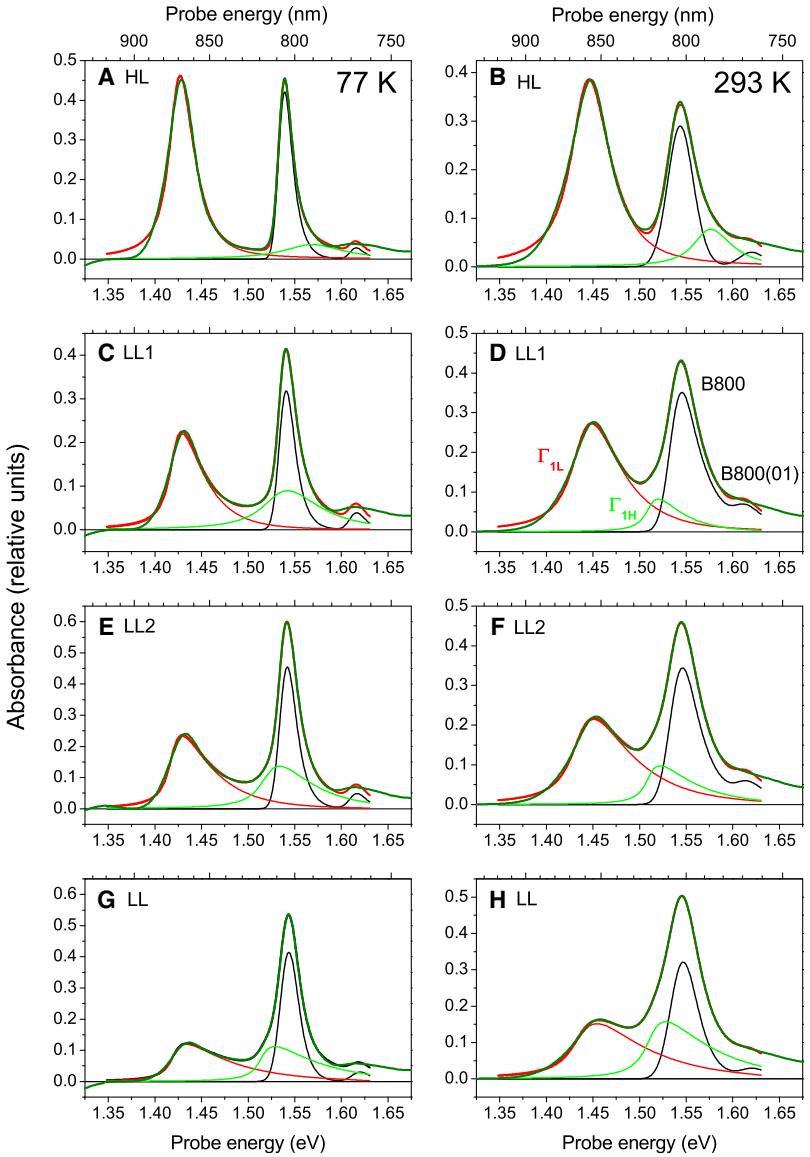

FIGURE 1 Ground state absorption spectra (*thick red lines*, normalized to BChl *a* Q_x band) as a function of growth conditions (*rows*) measured at two different temperatures (*left column*, 77 K; *right column*, 293 K). Thick green lines: calculated spectra according to the model explained in the text; thin red lines: calculated Γ_{1L}; thin green lines: calculated Γ_{1H}; thin black lines: molecular transition of Q_y band in B800 molecule including vibronic progression. See *D* for labeling of the transitions that is used in the text.

(compare Fig. 1, *A*, *C*, *E*, *G* and *B*, *D*, *F*, *H* for low and high temperature, respectively). Furthermore, Γ_{1L} becomes more asymmetric in the samples from cells grown at lower light intensities. As discussed below, it is a reasonable assumption that the apparent increase of both intensity and width of the B800 transition is in reality caused by a superposition of the (unchanged) B800 absorption with changes in the spectral properties in the B850 ring.

The absorption spectra of LH2 under all conditions were simulated using the following model: the B800 transition is regarded as a molecular transition together with its vibronic progression of one prominent normal mode; the B850 molecules form two excitonic bands, Γ_{1L} close to 1.43 eV (867 nm) and Γ_{1H} at 1.53 eV (810 nm). Both bands were assumed Lorentzian and inhomogeneous broadening was introduced by an exponential distribution with characteristic distribution energies of t_{800} for the B800 band and t_{850} for the one-exciton bands. Hereby, the distribution of states was assumed to decay exponentially toward higher energies.

The simulated spectra shown in Fig. 1 (*thick green lines*) closely reproduce the measured spectra (*thick red*). The individual contributions to the calculated spectra are shown as thin lines. The best fitting parameters as function of growth conditions are given in Table 1. Going from HL to LL, the ratio $r(\Gamma_{1H}/\Gamma_{1L})$ increases from 1:5 to nearly 1:1. This is a clear sign of a change in the B850 molecules, leading to a different excitonic splitting. The exponential broadening parameter t_{850} for the B850 excitonic features increases strongly under low light conditions, whereas it is only weakly temperature dependent. In contrast, the broadening t_{800} is not significantly dependent on the growth conditions but rather on the temperature. This clearly distinct behavior of the broadening parameters can be related to different

TABLE 1 Fitting parameters for the reproduction of ground state absorption spectra (Fig. 1) at 293 K

	HL	LL1	LL2	LL
E(B800)	1539 (1535)	1536 (1536)	1536 (1537)	1539 (1539)
$E(\Gamma_{1L})$	1439 (1422)	1437 (1421)	1435 (1419)	1436 (1421)
$E(\Gamma_{1H})$	1569 (1562)	1511 (1530)	1511 (1521)	1512 (1515)
$r(\Gamma_{1H}/\Gamma_{1L})$	0.20 (0.20)	0.21 (0.73)	0.34 (0.74)	0.90 (0.95)
t_{800}	6 (9)	24 (10)	21 (10)	14 (9)
t_{850}	11 (9)	25 (21)	38 (32)	50 (50)

All data are in meV except the ratio $r(\Gamma_{1H}/\Gamma_{1L})$, which has no unit. Values for 77 K are in parentheses.

broadening mechanisms affecting the monomeric and excitonic bands, respectively. According to the available literature, the B800 ring seems to be not influenced by growth conditions, so a dependence of the broadening parameter t_{800} on growth conditions is not expected (4,9,28). The temperature dependence of t_{800} can be assigned to dynamic disorder, caused by temperature-induced occupation of low-energetic intramolecular vibrational modes. The thermal occupation is governed by Boltzmann law, hence the exponential broadening (29).

Transition absorption spectra measurements

Pump-probe spectra of HL, LL, and two intermediate (LL1, LL2) samples of LH2 complexes from *Rps. palustris* were measured in the near infrared region to trace energy transfer and relaxation processes. Excited states in B800 were created by pumping at 795 nm (1.6 eV). An overall view of the pump probe spectra of LH2 samples (HL, LL1, LL2, and LL) is shown in the contour plots in Fig. 2, *A–D*, respectively. Photo-induced absorption (positive values, *red color*) progressively disappears when going from HL to LL samples; at the same time, the transient bleach (*green* and *blue*) of Γ_{1L} broadens. The changes in the higher energy region of pump-probe spectra point to the presence of a higher excitonic band in the LL LH2 exciton manifold. These features are also very clear in curves in Figs. 3 and 4 showing vertical and horizontal cuts of contour plots from Fig. 2. Fig. 3 shows pump-probe spectra at different pump-probe delay times, coded by color. In the case of the HL LH2 complexes (Fig. 3 *A*), at $t = 0$ (during the pump pulse), the spectrum shows the presence of a transient bleaching of both B800 and the Γ_{1L} ground state absorption bands, together with the excitonic state transition Γ_{L2}, i.e., from the lowest one-exciton level to the two-exciton level (30). The presence of excitonic B850-related features before energy transfer from B800 to B850 can be explained by a resonant generation of B850 excited states by the 1.6 eV pump pulse (Fig. 3 *A*, *black line*). Within 3 ps, the photobleaching signal from excited B800 completely disappears, whereas the photo-induced absorption (Γ_{L2}) and ground state bleaching (Γ_{1L}) of B850 increase strongly. This is a well known process and is due to energy transfer from B800 → B850. It is important to note that during this ET process, the increase of Γ_{1L} is much stronger than the concomitant bleaching recovery of B800. This clearly shows the excitonic nature of the B850. After 3 ps, no further spectral changes are observed in HL sample until much longer times (*magenta*, *yellow*, and *green* curves in Fig. 3 *A* are almost identical). All the curves in Fig. 3 *A* show a very clear isosbestic point at 1.44 eV that reflects the simple A → B reaction for ET from B800 to B850 in the absence of further spectral changes.

Pump-probe spectra of the LL samples at $t = 0$ are similar to those of the HL sample, compare Fig. 3, *B–D* to Fig. 3 *A*, respectively. The spectral evolution after the pump pulse is, however, dramatically different for the LL samples. The positive ΔA band at $t = 3$ ps decreases on going from LL1 to LL2, and no positive signal can be observed at all in the fully LL sample (Fig. 3, *magenta curves*). This loss of the positive band can be explained by superposition of positive

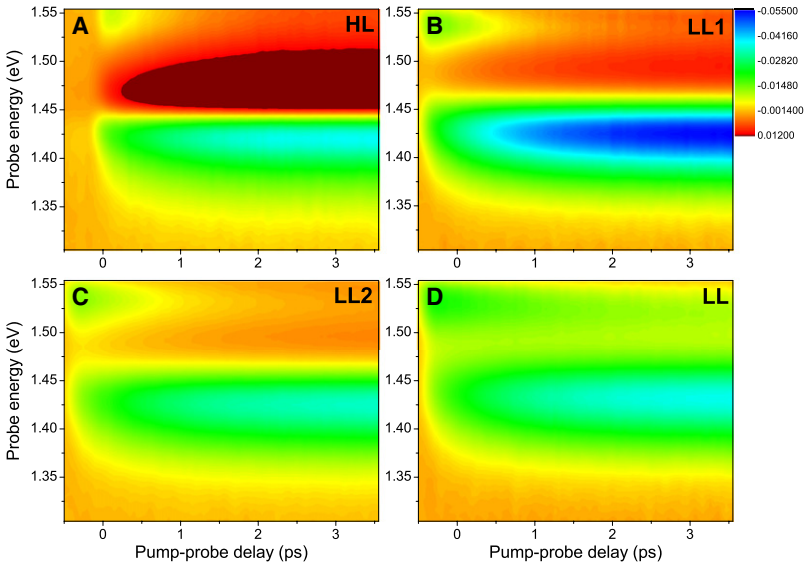

FIGURE 2 Contour plots of measured transient absorption spectra of LH2 complexes from *Rps. palustris* grown at four different illumination; changes in differential absorption (color scale is identical in all four panels) dependent on pump probe delay and probe energy are shown in (*A*) high light (HL), (*B* and *C*) two intermediate (LL1, LL2), and (*D*) low light (LL) sample, respectively. Red, photo-induced absorption; green and blue, transient bleach.

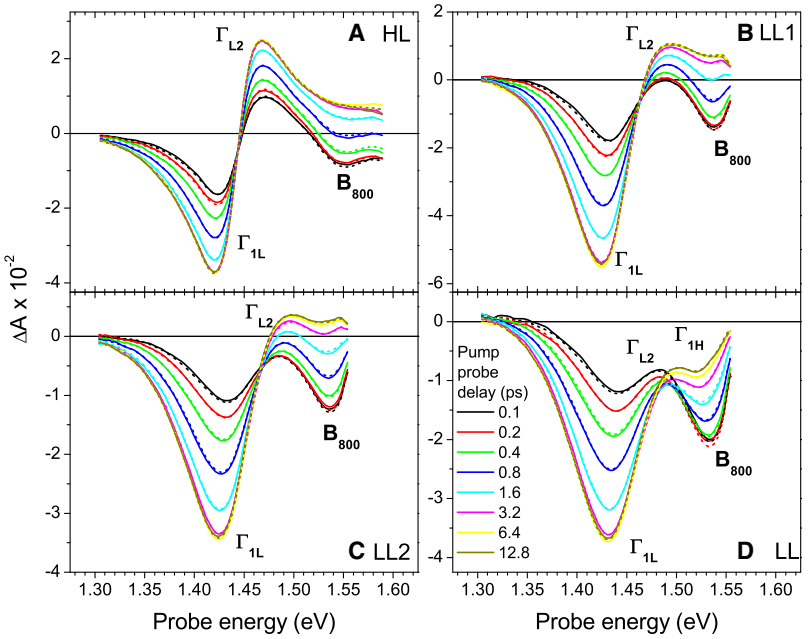

FIGURE 3 Differential absorption spectra of LH2 complexes at individual pump-probe delays. HL complex (*A*) shows Γ_{1L} transition, there is no change after 3.2 ps (*pink curve*), LL complex (*D*) presents an additional transition Γ_{1H} changing till ~10 ps (*yellow* and *olive curves*); panels of intermediate samples (*B*) LL1 and (*C*) LL2, respectively, represent increasing contribution of Γ_{1H} band to the spectra. All panels: solid lines, measured values; dashed lines, global fit.

and negative bands in close proximity. There is a positive Γ_{L2} band at 1.48 eV and a negative signal from the Γ_{1H} band, resulting in a local minimum at 1.53 eV. This provides evidence of a second, higher excitonic band of B850 in LL LH2 complexes in the region of 810 nm (Fig. 3 *D*). These findings are in agreement with the spectral assignment of the room temperature ground state absorption spectra (see Fig. 1). Finally, the positive (ΔA) band for the transition from the high-energy one-exciton band to the two-exciton band Γ_{H2} can be observed at 1.56 eV. In the lower light samples the presence of delayed kinetics is observed on the high energy side of the Γ_{1H} bleach (1.53 and 1.48 eV) (Fig. 3, *B–D*, *magenta* and *olive curves*). The shapes of the spectra on the low energy side are very similar for individual pump-probe delays (Fig. 3).

To illustrate more clearly the kinetics of the spectral evolutions in the LL samples, Fig. 4 presents time traces obtained as horizontal cuts through Fig. 2 at following probe energies: 1.35, 1.48, and 1.54 eV. In the HL sample, all time traces show mono-exponential behavior. In contrast, the LL samples show a clearly delayed contribution in the range from 1.48 to 1.54 eV, where several photo-induced features are superposed, namely B800, Γ_{L2}, and Γ_{1H}. In principle, the observed slow kinetics could be due to delayed ET from B800 to B850, causing a slow decrease of B800 and a concomitant slow build-up of the Γ_{L2} and Γ_{1H} transitions.

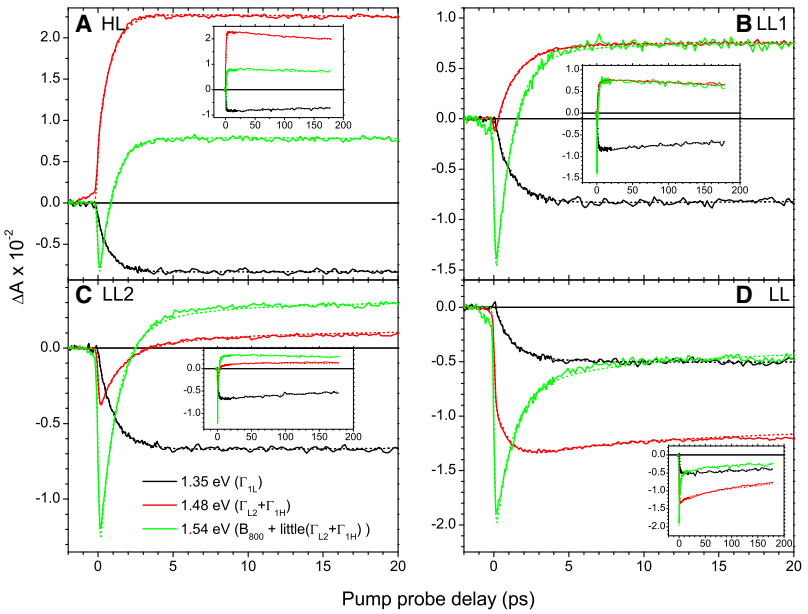

FIGURE 4 Time traces of differential absorption spectra of LH2 complexes from (*A*) HL, (*B*) LL1, (*C*) LL2, and (*D*) LL samples at three representative probe energies: 1.54 eV (805 nm), 1.48 eV (838 nm), and 1.35 eV (918 nm) (*green*, *red*, and *black lines*, respectively). Panels: processes from $t = 0$ until 20 ps; insets: processes until 200 ps. All panels: solid lines, measured values; dashed lines, global fit.

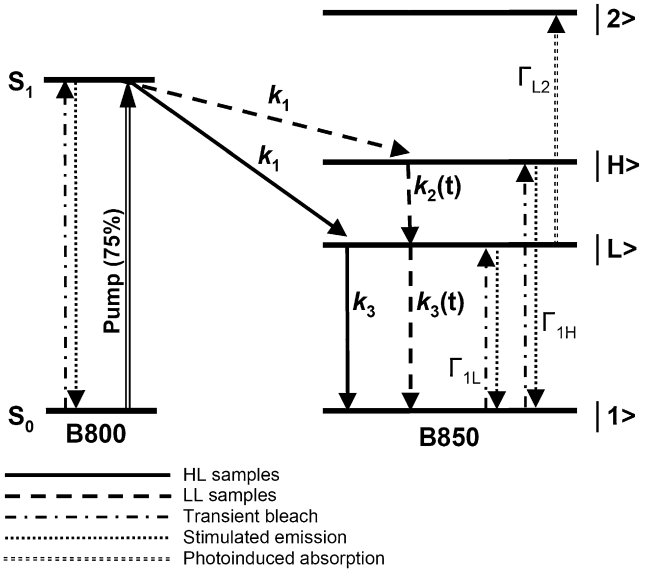

FIGURE 5 Photophysical model of energy transfer paths and associated rate constants between BChl *a* molecules in the B800 and the B850 ring. Processes for HL and LL samples are given as solid and dashed arrows, and the population probes that can be detected in transient absorption are given as dot-dashed and dotted lines.

However, no corresponding slow kinetic phase in the build-up of the Γ_{1L} bleach can be observed in time traces at 1.35 eV, where the signal is caused nearly exclusively by the Γ_{1L} transition (Fig. 4, *black lines*). Instead there is mono-exponential behavior for all samples. The picosecond spectral evolutions of B850 in the LL samples should therefore be associated with B850 exciton relaxation dynamics after B800 → B850 energy transfer. This picture is confirmed by a global fitting procedure (see below).

In the insets of Fig. 4, the same time traces are shown but on a longer timescale. It is evident that the decay of the B850 excitons to the ground state occurs significantly faster in the LL samples than in the HL sample. This difference is not due to exciton annihilation because in both cases the kinetics have been shown to be independent of the pump energy at pump intensities used here (data not shown). In LL samples, the forbidden transition from the B850 exciton back to the ground state is more allowed probably because of a disorder introduced into the LL LH2 structure due to the presence of different apoproteins (15).

ET rate constants for HL from global fitting

A global fitting procedure has been carried out to properly characterize the time-resolved measurements (see Materials and Methods for details). Perfect fits have been obtained for all measurements (Figs. 3 and 4, *dashed lines*). The fits are rationalized by a photophysical model that is shown in Fig. 5. For the HL sample, two basis spectra and two simple exponential rate constants are required. The first basis spectrum (Fig. 6 *A*, *dotted curve*) is assigned to the B800 excited state, created by resonant excitation by the pump pulse. The negative absorption feature at 1.55 eV is caused by transient bleaching of the respective ground state transition. The fitted absorption cross-section of this band is ~3 × 10^{-16} cm^2, which is close to the literature value of 2.3 × 10^{-16} cm^2 for this ground state transition (31). The first spectrum converts into the second spectrum in the process assigned to B800 → B850 energy transfer with decay constant k_1. The second basis spectrum (Fig. 6 *A*, *solid curve*) represents the excited state spectrum of the B850 exciton that decays with the rate constant k_3 to the ground state. It is characterized by a negative absorption band, centered at 1.42 eV,

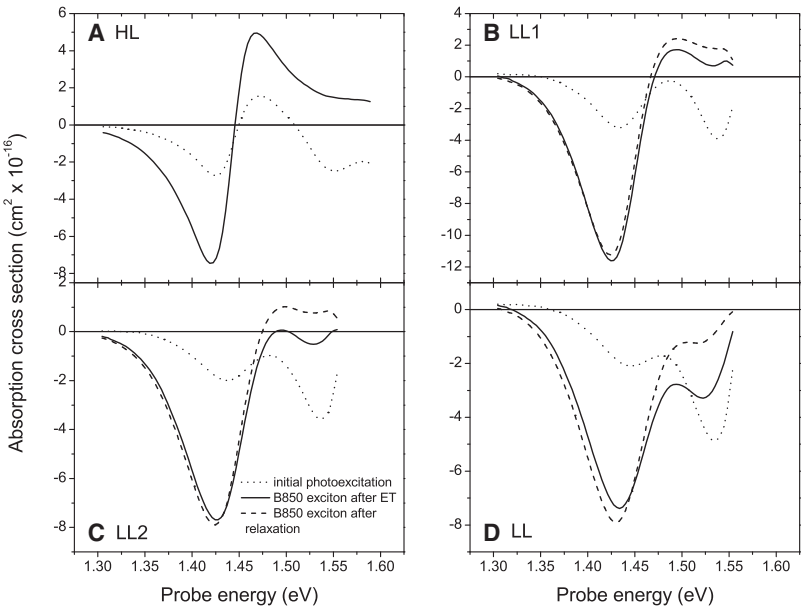

FIGURE 6 Photoexcitation spectra of LH2 complexes calculated by global fitting of pump probe spectra. Absolute absorption cross-section spectra are given for the initial, intermediate, and final photoexcitation (*dotted*, *solid*, and *dashed lines*, respectively) of (*A*) HL, (*B*) LL1, (*C*) LL2, and (*D*) LL complexes, respectively.

TABLE 2 Rate constants from global fitting of transient absorption spectra

Sample	$1/k_1$[†] (ps)	$1/k_2$[‡] (ps)	γ_2	$1/k_3$[§] (ps)	γ_3
HL	0.91	—	—	1 250	0*
LL1	1.10	2.00	−1.00	280	−0.16
LL2	1.00	1.60	−0.93	300	−0.16
LL	1.00	2.10	−0.94	220	−0.16

—, process not considered. Perfect fit obtained without this process, so inclusion was not justified.
*Value fixed.
[†]k_1 for energy transfer B800 → B850 is not dispersive.
[‡]k_2 for the process of exciton relaxation has the dispersive parameter γ_2.
[§]k_3 for exciton decay to the ground state with dispersive parameter γ_3.

and a positive absorption band at 1.47 eV. The observed transfer times $\tau_i = 1/k_i$ are in line with literature data where B800 → B850 transfer times of ~0.9 ps have been widely published for a variety of purple bacterial LH2 complexes (32–37). The shape of this second basis spectrum can be represented by a superposition of two Lorentzian bands of equal integral area, where the negative Lorentzian is centered at 1.45 eV, and the positive one at 1.46 eV (fit not shown). They are assigned to the Γ_{1L} and Γ_{L2} transitions, respectively. The slight blue-shift of the two-exciton transition versus the one-exciton transition is typical for strongly delocalized molecular excitons. From the lowest one-exciton state, the transition strength into higher exciton states is negligible because both transitions have equal oscillator strengths. This behavior is predicted for the $k = 0$ exciton (38). Because the resonance energy transfer from the B800 state should result in the creation of a hot, $k \neq 0$, exciton, it can be concluded that exciton relaxation is much faster than the B800 → B850 transfer rate, and cannot be observed in these time-resolved spectra. The values of the rate constants are summarized in Table 2. Interestingly, in Fig. 5, the dotted spectrum contains the same features as the solid one in the B850 region, compressed by roughly a factor of 3. It is possible to conclude that under current experimental conditions ~25% of the total B850 population is not created by energy transfer but by direct excitation.

Relaxation and dispersive decay of B850 excited states in LL samples

The absence of isosbestic points in Fig. 3 and the presence of slow transients in Fig. 4 suggest that more than two states are necessary for the global fit of the low light samples LL1, LL2, and LL. Indeed, for a good fit we need three basis spectra, coupled with three processes out of which the second and third ones are dispersive with time-dependent rate coefficients of the form $k_i(t) = k_i^0 \times (t/t_0)^{\gamma(i)}; i \in \{2,3\}; t_0 = 1$ ps. The fitted values are in Table 2. The basis spectra for the first photoexcitation (k_1, ET from B800–B850) are similar for LL and HL samples, containing contributions of both B800 bleach and B850 excitonic features (Fig. 6, *dotted curves*). In analogy to the HL sample, the first process is assigned

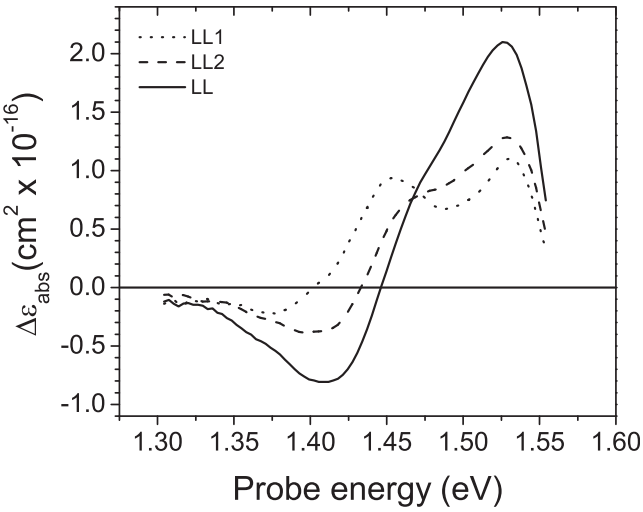

FIGURE 7 Differential spectra for LL, LL2, and LL1 samples (*solid*, *dashed*, and *dotted line*, respectively), calculated from second and third photoexcitation spectra. A clear signature of Γ_{1H} band in each LL sample and no change in B800 bleach contribution (no sign of delayed B800 → B850 ET) suggesting B850 exciton relaxation.

with the rate constant k_1 to B800 → B850 ET, and therefore the second basis spectrum represents the B850 exciton. Interestingly, the ET rate constant k_1 is only reduced by ~10% in LL samples with respect to the HL sample (Table 2). Because spectral overlap changes dramatically, this is strong evidence for a non-Förster type mechanism governing energy transfer (39).

By comparing the second and the third basis spectra, it is possible to characterize the slow spectral changes typical for low light samples. In contrast to the HL sample, the low light samples show a negative band at 1.53 eV. In agreement with Fig. 1, this band can be assigned to the Γ_{1H} transition, increasing in the order LL1 → LL2 → LL in both Figs. 1 and 6. The transition from the second to the third basis spectrum (Fig. 6, *dashed curves*) is characterized by a strong decrease of this Γ_{1H} transition, accompanied by a slight red-shift of the Γ_{1L} transition. The respective difference spectra are shown in Fig. 7 to show the differences between the second and third photoexcitation more clearly. In all cases, it is clear that the Γ_{1H} transition is weakened, and that there is no contribution of the B800 bleach to the observed spectral changes. This excludes the assignment of this process to a delayed ET from B800 → B850. According to the photophysical model suggested here and used for this analysis (Fig. 5), this process can be assigned to slow exciton relaxation from the initially populated higher exciton band (that is in resonance with B800 emission) to the lower one. If this is correct then it should be possible to observe the population transfer by a decrease of stimulated emission (SE) from the higher exciton, correlated with an increase of SE from the lower exciton. This is exactly what is observed in Fig. 6 *D*. The SE features occur slightly red-shifted against the bleaching, due to a small Stokes shift.

The observation of a time-dependent (dispersive) rate coefficient $k_2(t)$ in the low light samples supports its assignment to an exciton relaxation. The $k = 0$ exciton is reached via a cascade of intermediate steps, additionally superposed by vibronic relaxation (38). This sequence of elementary transfer steps with progressively increasing transfer times is the reason for the observed time-dependent relaxation coefficient. The possible reason for a much slower exciton relaxation in LL than in HL samples could be weaker electronic coupling between BChl *a* molecules in the LL B850 ring, where some of these molecules have B850-like and some others B820-like spectral properties due to a more complex apoprotein composition. In the LH2 complexes in general, the pigment binding apoproteins provide a quasi-continuum (bath) of states and the coupling of the BChl *a* to this bath causes fluctuations in the exciton energy. It has been pointed out that the coupling parameter (the amplitude of the bath-induced fluctuations of the Bchl *a* molecules) determines the time of exciton relaxation in different light harvesting systems. For LH1 complexes in *Blastochloris viridis*, a value of 490 cm^{-1} for this parameter has been obtained, resulting in a relaxation time below 100 fs (38). The loss of excitonic coherence in HL LH2 samples of *Rps. acidophila* strain 10050 has been measured to 160 fs (40). Justifying relaxation times in the picosecond time regime, as obtained here, requires a coupling term of <50 cm^{-1}. The bath in the case of the LH2 complexes consists of the many degrees of freedom of the binding apoproteins; the resulting dynamical fluctuations of atomic positions lead to a change in exciton splitting and/or site energies for the single BChl *a* molecules.

LH2 apoproteins versus spectral properties of B850 BChl a in LL

Previous studies have identified two key amino acid residues in LH2 α-apoprotein that are associated with the blue spectral shift of the B850 absorption band depending on light intensity during bacterial growth (4,8). In HL *Rps. acidophila*, Tyr^{44} and Trp^{45} form two hydrogen bonds that hold two carbonyl oxygen atoms in planar orientation with respect to the two B850 bacteriochlorin rings. In LH2 complexes isolated from *Rps. acidophila* strain 7050 grown at LL conditions, Tyr^{44} and Trp^{45} are replaced by Phe and Leu, respectively. Phe and Leu do not form hydrogen bonds with the carbonyl oxygens, leaving them out of the plane of the bacteriochlorin rings. This reorientation of the carbonyl groups results in lower degree of conjugation in the bacteriochlorin rings followed by the blue-shift of B850 band from 850 nm to 820 nm. When *Rps. palustris* is grown at LL one of the LH2 α-apoproteins that is expressed also has these 'key' amino acid residues replaced by Phe and Met (15). Under LL conditions, HL-type α-apoproteins are also expressed. This suggests that LL LH2 complexes could have BChl *a* molecules with mixed site-energies (both B820-like and B850-like) in the same individual LL LH2 complex. Indeed, in our experiments with LL LH2, both a higher exciton state Γ_{1H} and a lower exciton state Γ_{1L} have been observed. This result fits well with previous spectroscopic data that have been published suggesting the presence of mixtures of BChl *a* molecules with 'B820-like' and 'B850-like' site energies in one LH2 ring (12,16–18). Formally, this spectroscopic data does not distinguish between mixed rings and mixtures of different but homogenous B850 rings. However, a recent single molecule spectroscopic study on individual LL LH2 isolated from *Rps. palustris* provides direct proof that there are single LL LH2 complexes from *Rps. palustris* that do contain mixed rings (21). In this single molecule study, it was shown that in HL LH2 complexes, all exciton states where $k > 2$ are optically forbidden. In the case of LL LH2 complexes, the $k = 3$ exciton was significantly allowed, which explains the redistribution of oscillator strength toward higher energies seen in the absorption spectra of the LL complexes. In this analysis, the measurements represent an ensemble of energy bands, the single ($k = 1$, 2, and 3) exciton bands cannot be observed individually. Therefore, the decrease of oscillator strength toward higher energies is smooth and can be approximated by an exponential function that has been used in the kinetic model described above. It is not yet clear whether all the LL LH2 complexes have the same internal organization of the different antenna apoproteins that are present in the ensemble population. To help to answer this question more detailed quantitative analyses of the apoprotein composition are required.

CONCLUSIONS

Our study of LH2 complexes isolated from *Rps. palustris* grown at different light conditions has revealed what we believe to be novel characteristics of the ring of strongly coupled BChl *a* molecules in LL samples. In the case of HL LH2 complexes the spectroscopic properties of the B850 ring can be satisfactorily accounted for by assuming the presence of one major exciton band Γ_{1L}. In contrast, a second, higher energy exciton band Γ_{1H} is required to account for the properties of the LL LH2 complexes. The presence of the Γ_{1H} feature in the LL case is also supported by the decomposition analysis of the ground state absorption spectra of the LL samples.

The mono-exponential rate constant k_1 for ET from B800 to B850 is only slightly reduced (by ~10%) in LL samples in comparison to HL ones. The rate constant k_2 for the exciton relaxation from Γ_{1H} to Γ_{1L} is only seen in LL samples and is strongly dispersive. The decay of the B850 exciton back to ground state is faster in the LL samples by about a factor of 5, however, the decay remains very slow. The rate constant k_3 for this process is mono-exponential in the case of the HL complexes but is weakly dispersive in the LL ones. A simple photophysical model has been used to fully

reproduce the transient absorption spectra of LH2 complexes.

This work was supported by the European Commission (Marie Curie RTN BIMORE Program (MRTN-CT-2006-035859), the Energy Bioscience program of the Basic Energy Sciences division of the United States Department of Energy (DE-FG02-07ER15846 to R.E.B.), and from United States Department of Energy (DE- SC0001035), which established the Photosynthetic Antenna Research Center as a DOE Energy Frontier Research Center.

REFERENCES

1. Law, C. J., A. W. Roszak, J. Southall, A. T. Gardiner, N. W. Isaacs, et al. 2004. The structure and function of bacterial light-harvesting complexes. *Mol. Membr. Biol.* 21:183–191, [Review].
2. McDermott, G., S. M. Prince, A. A. Freer, A. M. Hawthornthwaite-Lawless, M. Z. Papiz, et al. 1995. Crystal-structure of an integral membrane light-harvesting complex from photosynthetic bacteria. *Nature*. 374:517–521.
3. Koepke, J., X. C. Hu, C. Muenke, K. Schulten, and H. Michel. 1996. The crystal structure of the light-harvesting complex II (B800–850) from *Rhodospirillum molischianum*. *Structure*. 4:581–597.
4. McLuskey, K., S. M. Prince, R. J. Cogdell, and N. W. Isaacs. 2001. The crystallographic structure of the B800–820 LH3 light-harvesting complex from the purple bacteria *Rhodopseudomonas acidophila* strain 7050. *Biochemistry*. 40:8783–8789.
5. Roszak, A. W., T. D. Howard, J. Southall, A. T. Gardiner, C. J. Law, et al. 2003. Crystal structure of the RC-LH1 core complex from *Rhodopseudomonas palustris*. *Science*. 302:1969–1972.
6. Cogdell, R. J., A. Gall, and J. Köhler. 2006. The architecture and function of the light-harvesting apparatus of purple bacteria: from single molecules to in vivo membranes. *Q. Rev. Biophys.* 39:227–324.
7. van Grondelle, R., and V. I. Novoderezhkin. 2006. Energy transfer in photosynthesis: experimental insights and quantitative models. *Phys. Chem. Chem. Phys.* 8:793–807.
8. Cogdell, R. J., T. D. Howard, N. W. Isaacs, K. McLuskey, and A. T. Gardiner. 2002. Structural factors which control the position of the Q(y) absorption band of bacteriochlorophyll a in purple bacterial antenna complexes. *Photosynth. Res.* 74:135–141.
9. Evans, M. B., A. M. Hawthornthwaite, and R. J. Cogdell. 1990. Isolation and characterization of the different B800–850 light-harvesting complexes from low-light and high-light grown cells of *Rhodopseudomonas palustris*, strain 2.1.6. *Biochim. Biophys. Acta*. 1016:71–76.
10. Hayashi, H., M. Miyao, and S. Morita. 1982. Absorption and fluorescence-spectra of light-harvesting bacteriochlorophyll-protein complexes from *Rhodopseudomonas palustris* in the near-infrared region. *J. Biochem.* 91:1017–1027.
11. Tadros, M. H., E. Katsiou, M. A. Hoon, N. Yurkova, and D. P. Ramji. 1993. Cloning of a new antenna gene-cluster and expression analysis of the antenna gene family of *Rhodopseudomonas palustris*. *Eur. J. Biochem.* 217:867–875.
12. Tadros, M. H., and K. Waterkamp. 1989. Multiple copies of the coding regions for the light-harvesting B800–850 alpha-polypeptide and beta-polypeptide are present in the *Rhodopseudomonas palustris* genome. *EMBO J.* 8:1303–1308.
13. Evans, K., A. P. Fordham-Skelton, H. Mistry, C. D. Reynolds, A. M. Lawless, et al. 2005. A bacteriophytochrome regulates the synthesis of LH4 complexes in *Rhodopseudomonas palustris*. *Photosynth. Res.* 85:169–180.
14. Vuillet, L., M. Kojadinovic, S. Zappa, M. Jaubert, J. M. Adriano, et al. 2007. Evolution of a bacteriophytochrome from light to redox sensor. *EMBO J.* 26:3322–3331.
15. Tharia, H. A., T. D. Nightingale, M. Z. Papiz, and A. M. Lawless. 1999. Characterization of hydrophobic peptides by RP-HPLC from different spectral forms of LH2 isolated from. *Rps. palustris*. *Photosynth. Res.* 61:157–167.
16. Gall, A., and B. Robert. 1999. Characterization of the different peripheral light-harvesting complexes from high- and low-light grown cells from *Rhodopseudomonas palustris*. *Biochemistry*. 38:5185–5190.
17. Georgakopoulou, S., R. N. Frese, E. Johnson, C. Koolhaas, R. J. Cogdell, et al. 2002. Absorption and CD spectroscopy and modeling of various LH2 complexes from purple bacteria. *Biophys. J.* 82:2184–2197.
18. van Mourik, F., A. M. Hawthornthwaite, C. Vonk, M. B. Evans, R. J. Cogdell, et al. 1992. Spectroscopic characterization of the low-light B800–850 light-harvesting complex of *Rhodopseudomonas palustris*, strain 216. *Biochim. Biophys. Acta*. 1140:85–93.
19. Hess, S., F. Feldchtein, A. Babin, I. Nurgaleev, T. Pullerits, et al. 1993. Femtosecond energy-transfer within the LH2 peripheral antenna of the photosynthetic purple bacteria *Rhodobacter sphaeroides* and *Rhodopseudomonas palustris* Ll. *Chem. Phys. Lett.* 216:247–257.
20. Nishimura, Y., K. Shimada, I. Yamazaki, and M. Mimuro. 1993. Energy-transfer processes in *Rhodopseudomonas palustris* grown under low-light conditions - Heterogeneous composition of LH-2 complexes and parallel energy-flow pathways. *FEBS Lett.* 329:319–323.
21. Brotosudarmo, T. H. P., R. Kunz, P. Böhm, A. T. Gardiner, V. Moulisová, et al. 2009. Single-molecule spectroscopy reveals that individual low-light LH2 complexes from *Rhodopseudomonas palustris* 2.1.6. have a heterogeneous polypeptide composition. *Biophys. J.* 97:1491–1500.
22. Böse, S. K. 1963. Bacterial Photosynthesis. Antioch Press, Yellow Springs, OH.
23. Cogdell, R. J., I. Durant, J. Valentine, J. G. Lindsay, and K. Schmidt. 1983. The isolation and partial characterization of the light-harvesting pigment-protein complement of *Rhodopseudomonas acidophila*. *Biochim. Biophys. Acta*. 722:427–435.
24. Polli, D., L. Luer, and G. Cerullo. 2007. High-time-resolution pump-probe system with broadband detection for the study of time-domain vibrational dynamics. *Rev. Sci. Instrum.* 78:103108.
25. van Stokkum, I. H. M., T. Scherer, A. M. Brouwer, and J. W. Verhoeven. 1994. Conformational dynamics of flexibly and semirigidly bridged electron donor-acceptor systems as revealed by spectrotemporal parameterization of fluorescence. *J. Phys. Chem.* 98:852–866.
26. Sauer, K., R. J. Cogdell, S. M. Prince, A. Freer, N. W. Isaacs, et al. 1996. Structure-based calculations of the optical spectra of the LH2 bacteriochlorophyll-protein complex from *Rhodopseudomonas acidophila*. *Photochem. Photobiol.* 64:564–576.
27. Zerlauskiene, O., G. Trinkunas, A. Gall, B. Robert, V. Urboniene, et al. 2008. Static and Dynamic Protein Impact on Electronic Properties of Light-Harvesting Complex LH2. *J. Phys. Chem. B*. 112:15883–15892.
28. Gardiner, A. T., R. J. Cogdell, and S. Takaichi. 1993. The effect of growth-conditions on the light-harvesting apparatus in *Rhodopseudomonas acidophila*. *Photosynth. Res.* 38:159–167.
29. Gierschner, J., H. G. Mack, L. Luer, and D. Oelkrug. 2002. Fluorescence and absorption spectra of oligophenylenevinylenes: vibronic coupling, band shapes, and solvatochromism. *J. Chem. Phys.* 116:8596–8609.
30. Novoderezhkin, V., R. Monshouwer, and R. van Grondelle. 1999. Disordered exciton model for the core light-harvesting antenna of *Rhodopseudomonas viridis*. *Biophys. J.* 77:666–681.
31. Connolly, J. S., E. B. Samuel, and A. F. Janzen. 1982. Effects of solvent on the fluorescence properties of bacteriochlorophyll A. *Photochem. Photobiol.* 36:565–574.
32. Herek, J. L., N. J. Fraser, T. Pullerits, P. Martinsson, T. Polívka, et al. 2000. B800 -> B850 energy transfer mechanism in bacterial LH2 complexes investigated by B800 pigment exchange. *Biophys. J.* 78:2590–2596.
33. Hess, S., E. Akesson, R. J. Cogdell, T. Pullerits, and V. Sundström. 1995. Energy transfer in spectrally inhomogeneous light-harvesting pigment-protein complexes of purple bacteria. *Biophys. J.* 69:2211–2225.
34. Ihalainen, J. A., J. Linnanto, P. Myllyperkio, I. H. M. van Stokkum, B. Ucker, et al. 2001. Energy transfer in LH2 of *Rhodospirillum*

molischianum, studied by subpicosecond spectroscopy and configuration interaction exciton calculations. *J. Phys. Chem. B*. 105:9849–9856.

35. Kennis, J. T. M., A. M. Streltsov, S. I. E. Vulto, T. J. Aartsma, T. Nozawa, et al. 1997. Femtosecond dynamics in isolated LH2 complexes of various species of purple bacteria. *J. Phys. Chem. B*. 101: 7827–7834.
36. Ma, Y. Z., R. J. Cogdell, and T. Gillbro. 1997. Energy transfer and exciton annihilation in the B800–850 antenna complex of the photosynthetic purple bacterium *Rhodopseudomonas acidophila* (Strain 10050). A femtosecond transient absorption study. *J. Phys. Chem. B*. 101:1087–1095.
37. Ma, Y. Z., R. J. Cogdell, and T. Gillbro. 1998. Femtosecond energy-transfer dynamics between bacteriochlorophylls in the B800–820 antenna complex of the photosynthetic purple bacterium *Rhodopseudomonas acidophila* (Strain 7750). *J. Phys. Chem. B*. 102:881–887.
38. Novoderezhkin, V., and R. van Grondelle. 2002. Exciton-vibrational relaxation and transient absorption dynamics in LH1 of *Rhodopseudomonas viridis*: a Redfield theory approach. *J. Phys. Chem. B*. 106:6025–6037.
39. Beljonne, D., C. Curutchet, G. D. Scholes, and R. J. Silbey. 2009. Beyond Förster resonance energy transfer in biological and nanoscale systems. *J. Phys. Chem. B*. 113:6583–6599.
40. Mercer, I. P., Y. C. El-Taha, N. Kajumba, J. P. Marangos, J. W. G. Tisch, et al. 2009. Instantaneous mapping of coherently coupled electronic transitions and energy transfers in a photosynthetic complex using angle-resolved coherent optical wave-mixing. *Phys. Rev. Lett.* 102:057402.